Low-cost Jacobian-free mapping for dynamic cell clustering in multi-regime reactive flows

Antoine Stock, Vincent Moureau, Julien Leparoux, Renaud Mercier

Low-cost Jacobian-free mapping for dynamic cell clustering in multi-regime reactive flows

Antoine Stock[a,*], Vincent Moureau[a], Julien Leparoux[b], Renaud Mercier[b]

[a] *CORIA, Normandie Univ, UNIROUEN, INSA Rouen, CNRS UMR6614, FRANCE*
[b] *Safran Tech, Digital Sciences Technologies Department, Rue des Jeunes Bois, Châteaufort, 78114, Magny-Les-Hameaux, FRANCE*

Abstract

Dynamic Cell Clustering (DCC), also referred as Cell Agglomeration, is an optimisation technique used to reduce the cost of finite-rate chemistry in reactive flows. It consists of three steps: i) grouping of elements with similar composition into clusters, ii) computation of a single element per cluster and iii) mapping of the computed elements to the remaining elements of the cluster through interpolation and extrapolation. The size of the clusters results from a compromise between cost reduction and desired accuracy. A new Jacobian-free mapping method (JFM) combined to Principal Component Analysis (PCA) is introduced in order to provide the accuracy of a higher-order mapping without the overhead of a Jacobian evaluation. The increased accuracy is obtained by creating a connectivity map between adjacent clusters. Along the cluster connections, composition and source term gradients are known enabling an approximation of the Jacobian. The JFM methodology is validated on a hydrogen-air triple flame, a multi-regime flame which covers a wide region in the species/temperature phase space. It is shown that for realistic clustering conditions the JFM method shows a similar accuracy to the explicit Jacobian. Compared to other mapping methods, an error reduction of up to 74% is observed while the cell agglomeration overhead remains less than 1% of the initial cost.

Keywords: Reactive flows; Dynamic Cell Clustering; Cell agglomeration; Principal Component Analysis; Jacobian-free mapping

Information for Colloquium Chairs and Cochairs, Editors, and Reviewers

1) Novelty and Significance Statement

A new mapping method for cell agglomeration is introduced. Prior methods have shown limitations in terms of efficiency or accuracy. The proposed Jacobian-Free Mapping (JFM) method combined with Principal Component Analysis for cell agglomeration is both accurate and efficient, no longer requiring a compromise between both properties. The method is original and performs very well for challenging multi-regime flames such as H2/air triple flames, which is of high interest for the decarbonation of the transport and energy sectors. As it is based on a Cartesian mapping and as it does not depend on the underlying chemical mechanism, it can be easily implemented in many codes and has a great potential for wide acceptance.

2) Author Contributions

- A. S. : performed research, implementation, paper writing
- V. M. : guided research, paper writing
- J. L. : guided research, paper writing
- R. M. : guided research, paper writing

3) Authors' Preference and Justification for Mode of Presentation at the Symposium

The authors prefer **OPP** presentation at the Symposium, for the following reasons:

- The presentation can focus on outcomes and results without requiring the inclusion of extensive background information
- A room-audience-level discussion about the proposed method would be profitable
- The proposed cell clustering method can be implemented in many codes, deserving a wide audience

1. Introduction

Reactive flows are a prominent subject of study, with applications spanning from combustion processes in engines to industrial reactors. Large-Eddy Simulation (LES) and Direct Numerical Simulations (DNS) have emerged as powerful tools for simulating turbulent reactive flows, providing valuable insights into the complex interactions between turbulence and chemical reactions. One of the primary challenges in unsteady modelling of reactive flows is the accurate computation of chemical source terms.

Finite-rate chemistry (FRC) is the most direct approach in combustion simulations. It involves solving a system of transport equations for each participating chemical species and calculating the rates of chemical reactions based on kinetic mechanisms. In reaction regions, chemical timescales can be several order of magnitude smaller than the flow timescales, thus requiring splitting approaches where chemistry is integrated separately from the flow. As a result, FRC offers precise representation of chemical processes but can become prohibitively expensive, particularly when increasing the size of kinetic schemes.

Several methodologies have been developed over the years to enhance the efficiency of solving chemistry. These methods include reducing kinetic schemes through advanced techniques such as DRGEP [1, 2], CSP [3], analytical reduction [4], and virtual chemistry [5]. Additionally, dynamic adaptive chemistry (DAC) [6, 7] offers the ability to perform on-the-fly kinetic mechanism reduction.

For a given kinetic scheme further gain can be achieved with chemistry tabulation [8]. Tabulation techniques are very popular and efficient but rely on the flamelet hypothesis and necessitate to precompute a look-up table based on canonical flames. Tabulation reaches its limits when departing from the flamelet regime or from the tabulated canonical flames. This can be overcome by storage-retrieval techniques like in-situ adaptive tabulation (ISAT) [9–11] or cell agglomeration techniques [12–17].

Cell agglomeration, also called Dynamic Cell Clustering (DCC) can be broken down into three steps: i) grouping of cells with similar composition into clusters, ii) computation of a single source term per cluster and iii) mapping of the computed cells towards remaining cells of the same cluster. This paper focuses on the mapping step and presents a new method that combines high accuracy and low computational cost. The use of Principal Components Analysis to create an optimal low-dimensional representation of the composition is also discussed. Section 2 presents the methodology and Section 3 validates the chosen approach on a H2/air triple flame.

2. Methodology

2.1. Cluster creation

Clustering methods aim at grouping similar computational cells together. Each cell acts as a chemical reactor, therefore clustering has to consider each parameter defining the reactor's behaviour. A common state vector is $\phi = \{P, T, Y_1, ..., Y_{Nsp}\}$, comprising the pressure, temperature and mixture composition. Further parameters could be required according to the combustion model: partially stirred reactors (PSR) or turbulent combustion models for instance.

2.1.1. Dimensionality reduction

To ease the clustering process, dimensionality reduction is performed on the species fractions. The most basic approach consists in retaining the most relevant species and ignoring the others. This requires user knowledge and is likely to result in a sub-optimal clustering. An alternative is Principal Component Analysis (PCA) [18, 19], which automatically creates an optimal low-dimensional representation of a mixture [20–22]. PCA identifies the principal components, which are linear combinations of the state variables. These combinations can be related to known properties such as a progress variable or mixture fraction. Mathematically, PCA involves finding the eigenvectors and eigenvalues of the covariance matrix of the input data. These eigenvectors represent the directions in the high-dimensional space along which the data varies the most, while the eigenvalues indicate the variance explained along each eigenvector. The low-dimensional representation of ϕ is referred to as M. In the current context only mass fractions are considered in the reduction, individual Principal Components are expressed as:

$$\begin{aligned} PC_i &= V_i Y \\ PC_i &= \sum_{k=1}^{N_{species}} V_{i,k} Y_k \end{aligned} \tag{1}$$

with V_i the ith eigenvector and $V_{i,k}$ the weight coefficients of individual species.

2.1.2. Clustering algorithm

K-Means [23] is one of the most popular and simplest clustering algorithms. It aims at partitioning data into K clusters, where each data point belongs to the cluster with the nearest mean value. It iteratively minimises the sum of squared distances between data points and their assigned cluster's centroid by moving the latter until an optimum is found. It has been used for cell agglomeration in [13]. An alternative approach is grid-based clustering [24]. This method divides the data space into a grid of cells. Each data point is then assigned to the grid cell that corresponds to its state coordinates. The goal is to group data points that fall within the same grid cell, effectively simplifying the clustering process and potentially making it more efficient for large datasets or

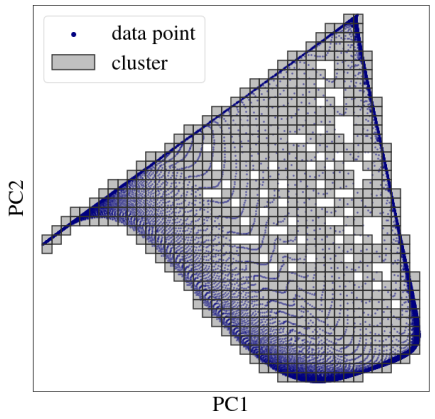

Fig. 1: Coarse clustering of data points along two dimensions of a H2-air triple flame

high cluster counts. A representation is given in figure 1. This method has been used for cell agglomeration in [12] and is chosen here for its efficiency.

2.2. Mapping

Once clusters have been formed and a single reactor computed, the result has to be mapped to all the elements within the cluster. As all elements have slightly distinct states, inevitably, errors are introduced when mapping the compositions. However, according to the choice of the mapping method, this error may be minimised. Backward mapping [14] consists in redistributing source term relative to mass fractions, while avoiding negative mass. This formulation is efficient but suffers from low accuracy and results in poor species gradients, as it will be shown in the validation section. Conversely, Jacobian-based mapping [16] has great accuracy but the computation of the Jacobian of a time-integrated chemical reactor is very expensive if not prohibitive.

This paper present a new mapping method, based on a Jacobian-free estimation. This estimation is designed to be low-cost while providing similar accuracy to an explicit Jacobian. Connectivity is created between the clusters, which is then used to approximate the Jacobian. Mapping is done based on those, while limiting degenerate cases.

2.2.1. Cluster connectivity

A connectivity map of adjacent clusters is created based on the cluster grid coordinates. Two clusters M_{C_1} and M_{C_2} are considered adjacent when they connect orthogonally:

$$\begin{aligned} &|M_{C_1,i} - M_{C_2,i}| = 1\,, \\ &M_{C_1,j} - M_{C_2,j} = 0 \quad \text{for all } j \neq i\,. \end{aligned} \tag{2}$$

An example of this connectivity, which can be computed efficiently using sparse matrices and sorting, is represented in Fig. 2. In this figure, the cluster center is the computed reactor, which is chosen as the one that minimizes composition difference $f(M_{\phi_i})$ to the other reactors:

$$f(M_{\phi_i}) = \sum_{j \neq i} \left\| M_{\phi_i} - M_{\phi_j} \right\|_2^2 . \tag{3}$$

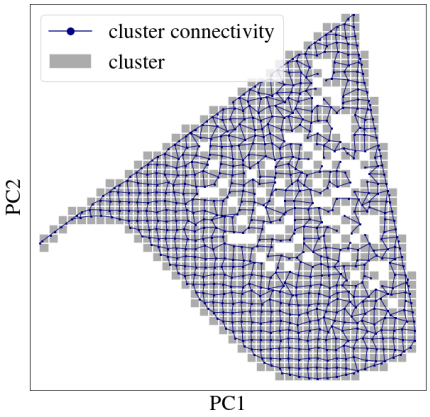

Fig. 2: Cluster connectivity based on computed reactor position based on Eq. 3

2.2.2. Jacobian-free mapping

Each edge of the connectivity graph allows to compute the Jacobian vector of the reaction rates within the reduced space M integrated along the edge. Let ϕ_{Ci} and ϕ_{Cj}, be the time-integrated reactors of two neighbour clusters C_i and C_j:

$$\phi_{Ci}^{t_0+\Delta t} = \phi_{Ci}^{t_0} + \dot{\omega}_i\,, \tag{4}$$

with $\dot{\omega}$ the source term. The source term difference between two adjacent clusters i and j is expressed as:

$$\Delta\dot{\omega}_{j\to i} = \dot{\omega}_i - \dot{\omega}_j\,. \tag{5}$$

Similarly, composition difference between clusters i and j is expressed as:

$$\Delta M_{j\to i} = M_{\phi_{Ci}^{t_0}} - M_{\phi_{Cj}^{t_0}}\,. \tag{6}$$

The ratio of those differences is first-order approximation of the Jacobian J_M projected onto the unit vector $dM_{j\to i}$.

$$J_M dM_{j\to i} \approx \frac{\Delta\omega_{j\to i}}{\Delta M_{j\to i}}\,. \tag{7}$$

Let ϕ_e be a reactor to be estimated within C_i, thus $\Delta\omega_{i\to e}$ needs to be estimated from the know displacement $\Delta M_{i\to e}$. Based on the knowledge of the Jacobian projected onto several known directions, the full Jacobian may be reconstructed and used to compute the change in the source terms:

$$\Delta\omega_{i\to e} = J_M \Delta M_{i\to e}\,. \tag{8}$$

However, degenerate cases can happen due to an insufficient number of projection directions or highly co-linear directions (see Sec. 3). Rather than computing the Jacobian at the cluster level, the source term variation can be expressed as a weighted sum of variations in known directions:

$$\Delta\omega_{i\to e} = \sum_{j=1}^{n} \alpha_j \Delta\omega_{i\to j}\,, \tag{9}$$

with n the number of connected clusters and α_j the interpolation coefficients to be determined from

$$\Delta M_{i\to e} = \sum_{j=1}^{n} \alpha_j \Delta M_{i\to j} = \mathcal{M}\alpha\,. \tag{10}$$

Eq. 10 can directly be inverted only if $n = d$, with d the number of dimensions of subspace M:

$$\alpha = \mathcal{M}^{-1}\Delta M_{i\to e}\,. \tag{11}$$

The case $n = 0$ is very unlikely as chemistry is continuous or is characteristic of an over-resolved clustering. This case is shared with other mapping methods. Solving for $1 \leq n < d$ may be obtained by a least square algorithm:

$$\alpha = \left(\mathcal{M}\mathcal{M}^t\right)^{-1}\mathcal{M}\Delta M_{i\to e}\,. \tag{12}$$

The least square returns α which minimises f:

$$f(\alpha) = \left\|\Delta M_{i\to e} - \mathcal{M}\alpha\right\|_2^2\,. \tag{13}$$

The obtained solution is the best possible projection of $\Delta M_{i\to e}$ given the insufficient amount of vectors in $\mathcal{M}$. This case is illustrated in Fig. 3a.

For $d < n$, Eq. 12 has an infinite number of solutions as there is an infinite number of vector combinations from $\mathcal{M}$ that are equal to $\Delta M_{i\to e}$. An additional constraint is set to obtain α with the smallest norm, which is expected to introduce minimal error. This is achieved with a least-square algorithm with ridge regression [25]:

$$\alpha = \left(\mathcal{M}\mathcal{M}^t + \lambda I\right)^{-1}\mathcal{M}\Delta M_{i\to e}\,. \tag{14}$$

The ridge regression returns α which minimises f:

$$f(\alpha) = \left\|\Delta M_{i\to e} - \mathcal{M}\alpha\right\|_2^2 + \lambda\left\|\alpha\right\|_2^2\,. \tag{15}$$

λ is chosen to be negligible compared to eigenvalues of $\mathcal{M}$ to not deteriorate the solution but way larger than machine accuracy to break the super-colinearity of the system. The constraint minimising the norm of α is optimal as it reduces extrapolation and thus error magnitude. Once α is found, degenerate cases have to be handled. It can be shown that Eq. 9 is an interpolation and not an extrapolation if and only if:

$$\begin{cases} \sum_{j=1}^{n} \alpha_j \leq 1\,, & (16) \\ \alpha_j \geq 0 \quad \text{for all } j \in \{1, ..., n\}\,. & (17) \end{cases}$$

Illustrations of these special cases are given in Figs. 3c and 3b. It will be shown that extrapolation is beneficial to some extent in Sec 3, however avoiding excessive extrapolations remains crucial. Rescaling of α may be introduced with a user-defined limit α_{lim}:

$$\alpha_{\text{rescaled}} = \frac{\alpha}{\max\left(1; \frac{\sum_{j=1}^{n}|\alpha_j|}{\alpha_{\text{lim}}}\right)}\,, \tag{18}$$

with typical values of α_{lim} ranging from 1 to 10.

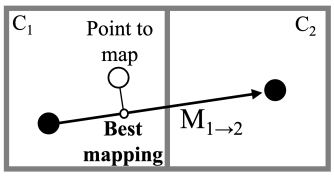

(a) Projection due to $n < d$.

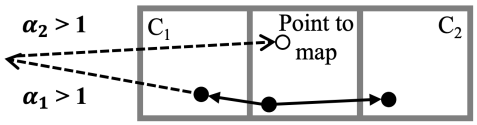

(b) Extrapolation due to violation of Eq. 16.

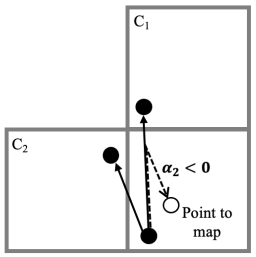

(c) Extrapolation due to violation of Eq. 17.

Fig. 3: Special cases for Jacobian-free mapping.

3. Validation

3.1. Simulation set-up

The implementation is done in YALES2 [26], which is a low-Mach number LES solver for massive unstructured meshes. Numerical methods are

4th-order in time and space and finite-rate chemistry is integrated with CVODE [27] with analytical Jacobian and full vectorization. PCA is performed with PETSc [28] using *dgesvd()*. A H_2-air triple flame [29, 30] in standard conditions is used as a reference case. It is solved using the San Diego mechanism [31], which counts 21 species and 64 reactions for H_2-air combustion with nitrogen chemistry. Inlet velocity is uniform and equal to $1m.s^{-1}$ and air-fuel equivalence ratio ranges from 0 to 24 to have non flammable conditions on the sides. This set-

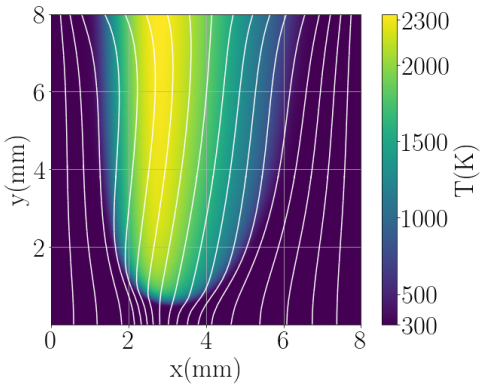

Fig. 4: Temperature field in the full simulation domain. Velocity streamlines are represented in white.

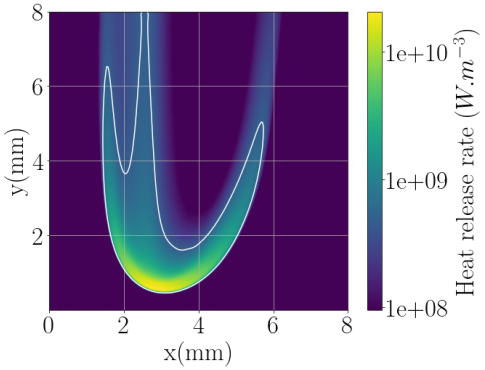

Fig. 5: Heat release rate (HRR) field in the full simulation domain with a HRR contour line to materialise the flame branches.

up is chosen as it spans a large region in the phase space with lean-premixed, rich-premixed and diffusive flame regimes altogether. The mesh, represented in Fig. 6, is refined within reactive areas thanks to feature-based mesh adaptation to limit the cost and the clustering of fresh gases.

3.2. Results

Error is measured on instantaneous quantities produced by the reactors: the Heat Release Rate (HRR)

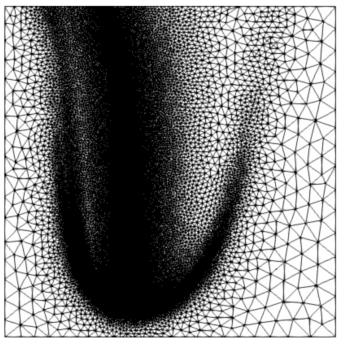

Fig. 6: Triple flame mesh, made of 50'000 elements with smallest elements size of 20 microns.

and the species source terms $\dot{\omega}_k$ related by:

$$HRR = \sum_{k=1}^{N_{species}} \dot{\omega}_k H^0_{f,k}\,, \tag{19}$$

with $H^0_{f,k}$ the standard enthalpy of formation of species k. The analysis is focused on HRR here but the same conclusions are obtained for individual species. Within a solver iteration, reactors are solved twice, with and without clustering, computation is advanced based on the reference without clustering. Relative error is obtained based on the integrated difference:

$$E = \frac{\sum_{i=1}^{N_{\text{elem}}} |HRR_{\text{cluster},i} - HRR_{\text{ref},i}|\, V_i}{\sum_{i=1}^{N_{\text{elem}}} |HRR_{\text{ref},i}|\, V_i}\,. \tag{20}$$

Measurement of the error is started from a quasi-steady state of the triple flame. The error should tend to zero when the size of the clusters ε is reduced. Fig. 7 shows this behaviour when varying the clustering dimensions.

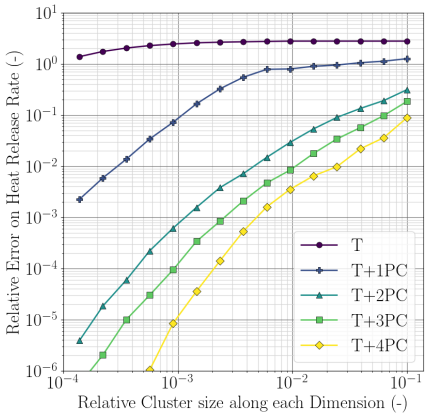

Fig. 7: Relative error on heat release rate relative to cluster resolution.

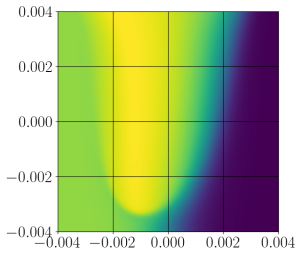

(a) PC1 field

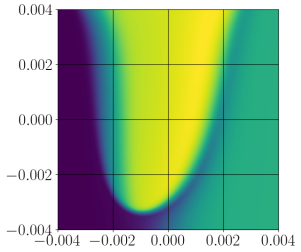

(b) PC2 field

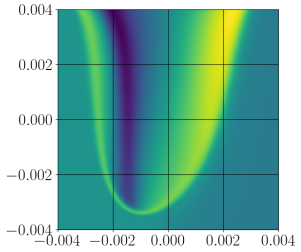

(c) PC3 field

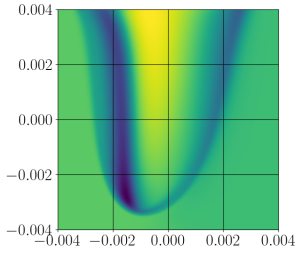

(d) PC4 field

Fig. 8: Normed Principal Component fields of the triple flame

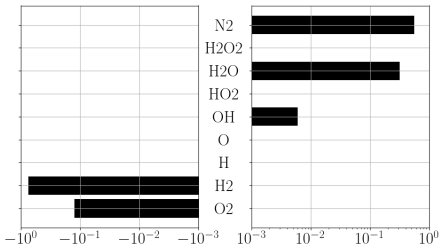

(a) PC1 coefficients

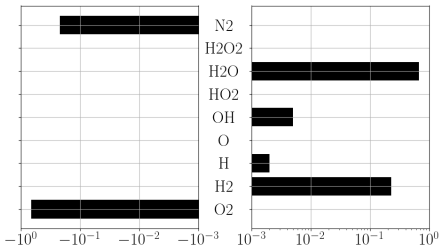

(b) PC2 coefficients

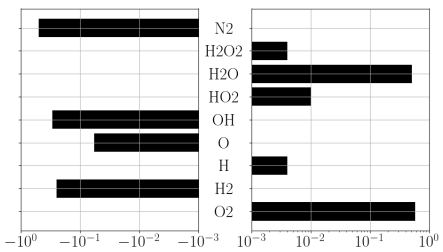

(c) PC3 coefficients

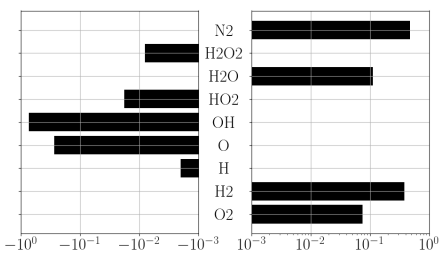

(d) PC4 coefficients

Fig. 9: Principal Component coefficients of the triple flame

Principal Components of the triple flame are shown in Fig. 8 and Fig. 9 and their variance, i.e. fluctuations of composition is given in Tab. 1.

Using only T or $T + PC1$ is insufficient as the relative error on HRR remains higher than relative cluster size. When advanced with clustering, these cases diverge, unless cluster resolution is extremely high.

	Variance	Cumulated Variance
PC1	0.7526	0.7526
PC2	0.2454	0.9980
PC3	0.0015	0.9995
PC4	0.0004	0.9999

Table 1: Normalized variance along the 4 first principal components. All simulation points are considered here.

Using 2 PC or more is satisfactory, which is consistent as the two first PC hold most of the explained variance. When advanced with clustering these cases show great stability unless cluster resolution is extremely coarse.

Clustering along Principal Components with little variance, like PC3 and PC4 is sub-optimal as way more reactors need to be solved for a small error decrease. This is investigated by introducing a reduced computational time:

$$RCT = \frac{\text{Wall clock time}(\mu s).N_{\text{cores}}}{N_{\text{elements}}.N_{\text{iterations}}}. \qquad (21)$$

Fig. 10 shows the relation between HRR error and RCT. As previously, T and $T + 1PC$ have poor performance. $T + 2PC$, $T + 3PC$ and $T + 4PC$ have very similar behaviour. $T + 4PC$ becomes slightly more expensive at high cluster resolution due to some excessive clustering.

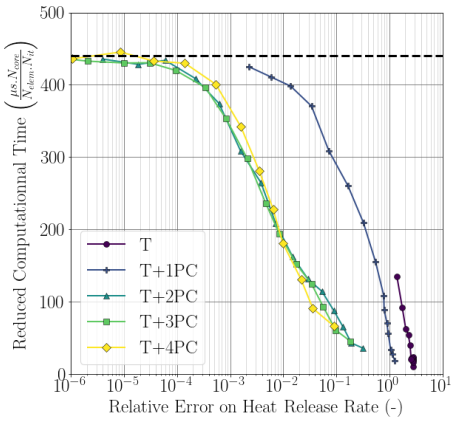

Fig. 10: RCT of source term computation depending on the number of Principal Components. Dashed line represents the reference cost without cell agglomeration.

The Jacobian-free mapping is now considered using two Principal Components. An accuracy comparison between backward, Jacobian and Jacobian-free mapping is performed in Fig. 11. As expected Jacobian mapping is at all times more accurate than backward mapping. On large clusters, the Jacobian-free mapping has a higher accuracy than the explicit Jacobian. This is because it is computed based on a variation of cluster size, thus filtering most of the high-frequency non-linear species production rates. On small cluster size the accuracy of the Jacobian-free mapping drops to the level of the backward mapping due to a lack of connectivity. It should be noted that clustering is most likely to be used with relatively large cluster sizes.

Performance of the Jacobian-free mapping is given by Fig. 12. Jacobian performance is not shown as an efficient implementation is not trivial. In the current study its evaluation cost exceeds by far the source

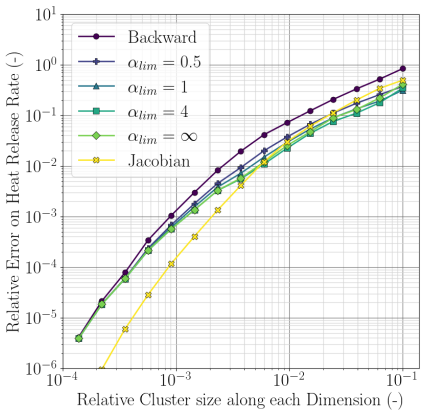

Fig. 11: Accuracy comparison between backward, Jacobian and Jacobian-free mapping.

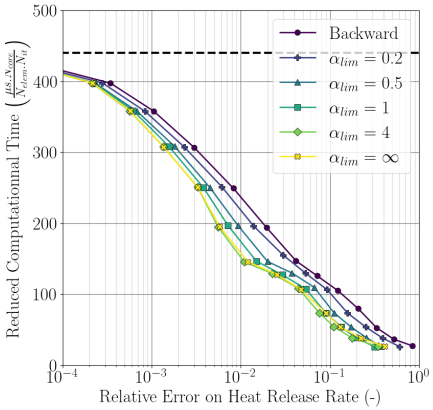

Fig. 12: RCT of source term computation versus α_{lim}.

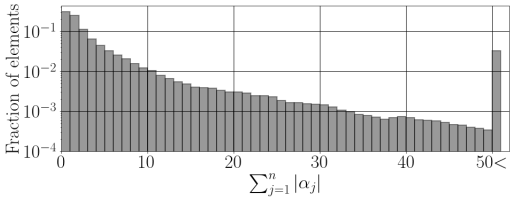

Fig. 13: Values of α per mapped element at $\epsilon = 0.01$.

term computation cost. At equivalent RCT, error is diminished by up to 74% using Jacobian-free mapping. Best results are obtained when extrapolation is used at $\alpha_{lim} = 4$ but larger extrapolation deteriorate the solution. This is also clearly shown by HRR fields of Fig. 14. While $\alpha_{\text{lim}} = 4$ provides a smoother and more realistic solution than backward mapping, using extrapolation without a limiter can create extremely sharp local errors. Fig. 13 also stresses the need for a limiter by showing that a few elements can reach

prohibitive values of α, reaching a magnitude of over 1000.

Overhead induced by the cell agglomeration remains less than 1% of the initial source term cost and is given in Tab. 2. Largest cost is associated with PCA. It should be noted that this is the cost if PCA was to be performed at every single iteration, which is not needed in most combustion cases. The cluster creation cost is negligible as it mainly relies on radix sort, which is very efficient on integers. Mapping cost consists mainly in solving the ridge regression while creation of connectivity is negligible.

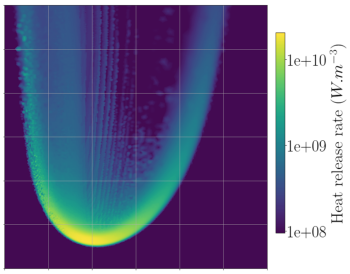

(a) backward

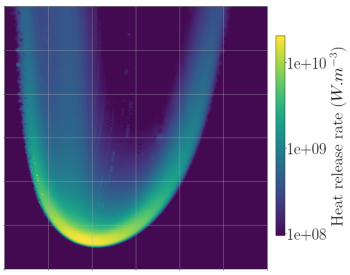

(b) $\alpha_{\text{lim}} = 4$

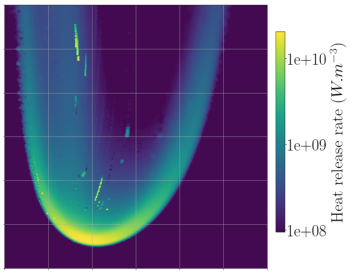

(c) $\alpha_{\text{lim}} = \infty$

Fig. 14: HRR field depending on α at $\epsilon = 0.01$.

Reference run	RCT	%
Source terms	440.0	100.00
Cell agglomeration	RCT	%
Source terms	122.1	27.80
+ PCA	1.8	0.41
+ Clustering	0.3	0.07
+ Mapping	1.1	0.25

Table 2: Source term cost and cell agglomeration overheads at $\epsilon = 0.01$.

4. Conclusions

A new mapping method for cell agglomeration has been introduced. Its accuracy and cost-reduction has been demonstrated in a challenging hydrogen-air triple flame. While the methodology parallelism has not been discussed here, cell agglomeration can be easily performed in parallel for partitioned domains, with each core having its own clusters. Future investigations should therefore be focused on massive DNS and LES of turbulent flames.

Declaration of competing interest

The authors declare that they have no known competing financial interests or personal relationships that could have appeared to influence the work reported in this paper.

Acknowledgments

This work has received funding from the European Union's Horizon 2020 research and innovation programme under the CoEC project, grant agreement No 952181. Access to the HPC resources of TGCC and IDRIS was granted under the allocations 2023-A0142A11335 and 2023-A0152B06880 made by GENCI.

References

[1] T. Lu, C. K. Law, A directed relation graph method for mechanism reduction, Proceedings of the Combustion Institute 30 (1) (2005) 1333–1341. doi:10.1016/j.proci.2004.08.145.

[2] P. Pepiot-Desjardins, H. Pitsch, An efficient error-propagation-based reduction method for large chemical kinetic mechanisms, Combustion and Flame 154 (1-2) (2008) 67–81. doi:10.1016/j.combustflame.2007.10.020.

[3] M. Valorani, F. Creta, D. A. Goussis, J. C. Lee, H. N. Najm, An automatic procedure for the simplification of chemical kinetic mechanisms based on CSP, Combustion and Flame 146 (1-2) (2006) 29–51. doi:10.1016/j.combustflame.2006.03.011.

[4] Q. Cazères, P. Pepiot, E. Riber, B. Cuenot, A fully automatic procedure for the analytical reduction of chemical kinetics mechanisms for Computational Fluid Dynamics applications, Fuel 303 (11 2021). doi:10.1016/j.fuel.2021.121247.

[5] M. Cailler, N. Darabiha, D. Veynante, B. Fiorina, Building-up virtual optimized mechanism for flame modeling, Proceedings of the Combustion Institute 36 (1) (2017) 1251–1258. doi:10.1016/j.proci.2016.05.028.

[6] D. A. Schwer, P. Lu, W. H. Green, An adaptive chemistry approach to modeling complex kinetics in reacting flows, Combustion and Flame 133 (4) (2003) 451–465. doi:10.1016/S0010-2180(03)00045-2.

[7] L. Liang, J. G. Stevens, J. T. Farrell, A dynamic adaptive chemistry scheme for reactive flow computations, Proceedings of the Combustion Institute 32 I (1) (2009) 527–534. doi:10.1016/j.proci.2008.05.073.

[8] E. Knudsen, H. Pitsch, Capabilities and limitations of multi-regime flamelet combustion models, Combustion and Flame 159 (1) (2012) 242–264. doi:10.1016/j.combustflame.2011.05.025.

[9] S. B. Pope, Computationally efficient implementation of combustion chemistry using in situ adaptive tabulation, Combustion Theory and Modelling 1 (1) (1997) 41–63. doi:10.1080/713665229.

[10] L. Lu, S. B. Pope, An improved algorithm for in situ adaptive tabulation, Journal of Computational Physics 228 (2) (2009) 361–386. doi:10.1016/j.jcp.2008.09.015.

[11] B. J. Liu, S. B. Pope, The performance of in situ adaptive tabulation in computations of turbulent flames, Combustion Theory and Modelling 9 (4) (2005) 549–568. doi:10.1080/13647830500307436.

[12] G. M. Goldin, Z. Ren, S. Zahirovic, A cell agglomeration algorithm for accelerating detailed chemistry in CFD, Combustion Theory and Modelling 13 (4) (2009) 721–739. doi:10.1080/13647830903154542.

[13] F. Perini, High-dimensional, unsupervised cell clustering for computationally efficient engine simulations with detailed combustion chemistry, Fuel 106 (2013) 344–356. doi:10.1016/j.fuel.2012.11.015.

[14] L. Liang, J. G. Stevens, J. T. Farrell, A dynamic multi-zone partitioning scheme for solving detailed chemical kinetics in reactive flow computations, Combustion Science and Technology 181 (11) (2009) 1345–1371. doi:10.1080/00102200903190836.

[15] A. Babajimopoulos, D. N. Assanis, D. L. Flowers, S. M. Aceves, R. P. Hessel, A fully coupled computational fluid dynamics and multi-zone model with detailed chemical kinetics for the simulation of premixed charge compression ignition engines, International Journal of Engine Research 6 (5) (2005) 497–512. doi:10.1243/146808705X30503.

[16] Q. Xie, Y. Liu, M. Yao, H. Zhou, Z. Ren, A fully coupled, fully implicit simulation method for unsteady flames using Jacobian approximation and clustering, Combustion and Flame 245 (11 2022). doi:10.1016/j.combustflame.2022.112362.

[17] A. Cuoci, A. Nobili, A. Parente, T. Grenga, Tabulation-based sample-partitioning adaptive reduced chemistry and cell agglomeration, Tech. rep.

[18] Jolliffe I. T., Principal Component Analysis , Springer New York, NY, 2002.

[19] H. Hotelling, Analysis of a complex of statistical variables into principal components, Tech. rep. (1930).

[20] J. C. Sutherland, A. Parente, Combustion modeling using principal component analysis, Proceedings of the Combustion Institute 32 I (1) (2009) 1563–1570. doi:10.1016/j.proci.2008.06.147.

[21] K. Zdybał, G. D'Alessio, G. Aversano, M. R. Malik, A. Coussement, J. C. Sutherland, A. Parente, Advancing Reacting Flow Simulations with Data-Driven Models (9 2022).

[22] Y. Yang, S. B. Pope, J. H. Chen, Empirical low-dimensional manifolds in composition space, Combustion and Flame 160 (10) (2013) 1967–1980. doi:10.1016/j.combustflame.2013.04.006.

[23] J. Macqueen, Some methods for classification and analysis of multivariate observations, Tech. rep., University of California, Los Angeles (1967).

[24] Gan Guojun, Ma Chaoqun, Wu Jianhong, Grid-based Clustering Algorithms, Data clustering: Theory, Algorithms, and Applications 6 (12) (2017) 209–2017. doi:10.1137/1.9780898718348.ch12.

[25] Arthur E. HOERL, Robert W. KENNAR, Ridge Regression: Biased Estimation for Nonorthogonal Problem, Tech. Rep. 1, University of Delaware and E. I. du Pont de Nemours & Co (2000).

[26] V. Moureau, P. Domingo, L. Vervisch, Design of a massively parallel CFD code for complex geometries (2 2011). doi:10.1016/j.crme.2010.12.001.

[27] Cohen D, Hindmarsh A, CVODE, A Stiff/Nonstiff ODE Solver in C, Computers in Physics 10 (2) (1996) 138–143.

[28] Satish Balay, Shrirang Abhyankar, Mark˜F. Adams, PETSc Web page (2023).

[29] J. W. Dold, Flame Propagation in a Nonuniform Mixture: Analysis of a Slowly Varying Triple Flame, Tech. rep. (1989).

[30] Veynante D, Vervisch L, Poinsot T, Linan A, Ruetsch G, Triple flame structure and diffusion flame stabilization, Center for turbulent research, Proceedings of the Summer Program (1994).

[31] "Chemical-Kinetic Mechanisms for Combustion Applications", San Diego Mechanism web page, Mechanical and Aerospace Engineering (Combustion Research), University of California at San Diego.